Vol 16 No 1, January 2007
1009-1963/2007/16(01)/0095-05

Chinese Physics

© 2007 Chin. Phys. Soc.
and IOP Publishing Ltd

# The influence of nickel dopant on the microstructure and optical properties of $SnO_2$ nano-powders*

Liu Chun-Ming(刘春明)[a], Fang Li-Mei(方丽梅)[a],
Zu Xiao-Tao(祖小涛)[a)b)†], and Zhou Wei-Lie(周伟列)[c]

[a] *Department of Applied Physics, University of Electronic Science and Technology of China, Chengdu* 610054, *China*
[b] *International Center for Material Physics, Chinese Academy of Sciences, Shenyang* 110015, *China*
[c] *Advanced Materials Research Institute, University of New Orleans, New Orleans LA* 70148, *USA*

(Received 22 February 2006; revised manuscript received 21 July 2006)

The microstructure and optical properties of Ni-doped $SnO_2$ nano-powders are studied in detail. By Ni-doping, not only the grain size reduces, but also the grain shape changes from nano-rods to spherical particles. The crystallization becomes better with annealing temperature increasing. The band gap energy decreases as nickel doping level increases. The sp–d hybridization and alloying effect due to amorphous $SnO_{2-x}$ phase should be responsible for the band gap narrowing effect. Nickel dopant does not change the photoluminescence (PL) peak positions.

**Keywords:** microstructure, optical absorption spectra, photoluminescence spectra, $SnO_2$

**PACC:** 4225

## 1. Introduction

As a chemical stable n-type semiconductor with a wide band gap energy, rutile-type tin dioxide ($SnO_2$) is known to have a wide range of technological applications, such as gas sensors[1] and transparent conducting electrodes,[2] and much attention has been paid to the photoluminescence properties of $SnO_2$.[3−7] The electrical and optical properties of $SnO_2$ can be largely modified by dopants. Up to now, $SnO_2$ has been doped separately with group III, V, VI and VII elements of the periodic table such as In, Ti, P, As, Sb, Te, F, Cl, Br and I to modify these properties.[8−11] Recently, $SnO_2$ doped with 3d-transition metals has displayed some interesting magnetic properties and attracted great attention.[12−15] It is well known that the presence of the magnetic ion in a compound semiconductor leads to a number of novel electronic and optical properties, such as the d–d optical absorption due to the strong coulomb interaction between the 3d electrons and band gap modification by sp–d hybridization.[16,17] However, to author's knowledge there is no report on the optical properties of the nickel-doped $SnO_2$ although a great effort has been made to study it as gas sensors.[18,19] In this paper we present the influence of nickel dopant on the microstructure and optical properties of $SnO_2$ nano-powders.

## 2. Experiments

Ni-doped $SnO_2$ nano-powders were successfully prepared by means of dissolving tin chloride (hydrous $SnCl_4 \cdot 5H_2O$(A.R.)) and nickel chloride (hydrous $NiCl_2 \cdot 6H_2O$(A.R.)) in distilled water. In a typical synthesis, an aqueous ammonia solution was added to the above solution dropwise. The dropping rate must be well controlled for the chemical homogeneity. The resulting gels were collected, washed in distilled water, and then dried at 100 °C for several hours. Heating treatment of the synthesized nano-powders was conducted in air for 1 h separately at each of the following temperatures: 350 °C, 400 °C, 500 °C, 650 °C and 800 °C.

The crystalline structure of the material was analysed by x-ray diffraction (XRD) using a Rigaku D/max-2400 diffractometer with curved crystal

*Project supported by the NSAF Joint Foundation of China (Grant No 10376006), the Program for New Century Excellent Talents in University of China (Grant No NCET-04-0899), the Ph.D. Funding Support Program of Education Ministry of China.
†Corresponding author. E-mail: xiaotaozu@yahoo.com

monochromator and CuK$\alpha$ radiation (= 0.154056 nm) operated at 40 kV and 60 mA. The sample stoichiometry was measured by a KRATOS X SAM 800 x-ray photoelectron spectroscopy (XPS). The feature micrographs were obtained using the H-600 transmission electron microscopy (TEM) operated at 100 kV. After the as-produced powders were well dispersed in distilled water suspension by using a supersonic disperser, the absorption spectra of the samples were measured using a Shimadzu UV-2500 UV–Visible spectrophotometer. The photoluminescence (PL) spectra were measured with a Shimadzu RF-5301PC spectrofluorophotometer.

## 3. Results and discussion

XRD patterns of $Sn_{1-x}Ni_xO_2$ (with $x = 0$, 0.02 and 0.05) annealed at 350 °C for 1 h are shown in Fig.1, in which (a), (b) and (c) correspond to $x = 0$, 0.02 and 0.05, respectively.

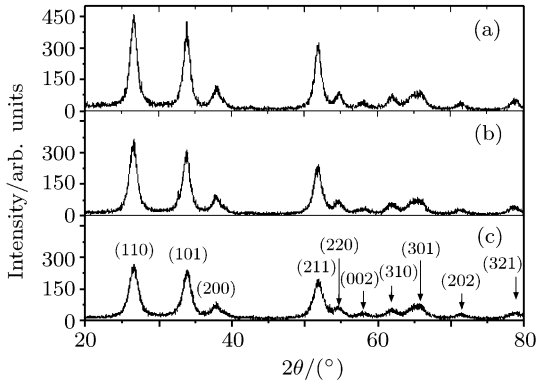



**Fig.1.** XRD patterns of $Sn_{1-x}Ni_xO_2$, with (a) $x = 0$, (b) $x = 0.02$, and (c) $x = 0.05$, respectively.

The diffraction indices are indicated in Fig.1(c). As seen in Fig.1, x-ray diffraction measurements reveal that the structures of all the samples are of rutile-type cassiterite (tetragonal) phase of $SnO_2$, and the doping does not change the tetragonal structure of $SnO_2$. Furthermore, we cannot find any traces of impurity, at least from the XRD data. The peak positions do not show any measurable changes, while the intensities of the peaks decrease with Ni content increasing. As Ni content increases, the XRD peaks become wider, indicating possible changes in the crystallite size and / or strain. This is similar to that reported in Ref.[15]. Using the Scherrer equation, the crystal size can be estimated. The crystal sizes determined by (110) diffraction peak are 8, 7 and 6 nm for $x = 0$, 0.02 and 0.05, respectively. It is evident that the introducing of nickel dopant inhibits their crystallization.

In order to investigate the dependence of crystalline structure on the annealing temperature, XRD patterns of the sample with $x = 0.02$ annealed at different temperatures for 1 h are shown in Fig.2.

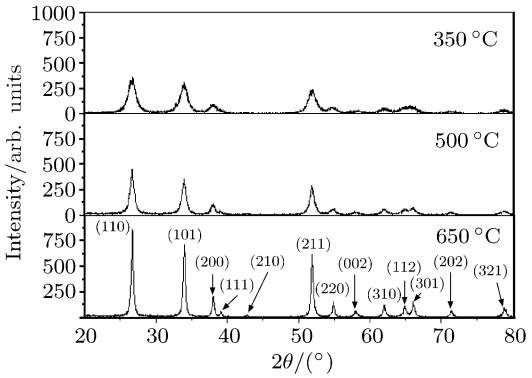



**Fig.2.** XRD patterns of $Sn_{0.98}Ni_{0.02}O_2$ annealed at different temperatures.

With the increase of annealing temperature, the full width at half maximum (FWHM) of the peak decreases and the intensity of the peak increases obviously, which shows that the size of the grain becomes larger and the structure of the lattice becomes better. For the lower annealing temperatures, the obtained samples are of imperfect lattice structure and have smaller grain sizes. For the tetragonal structure, the lattice parameters can be calculated from

$$\frac{1}{d_{hkl}^2} = \frac{h^2 + k^2}{a^2} + \frac{l^2}{c^2}, \tag{1}$$

where $h$, $k$, and $l$ are all integers, $(hkl)$ is the lattice plane index, and $a$ and $c$ are lattice constants. The obtained lattice constants are presented in Table 1, in which $a$ and $c$ are calculated from XRD peaks (110) and (101), $\Delta\alpha$ and $\Delta c$ are the differences between the measured lattice constant and that of the standard $SnO_2$ for $a = 4.738$ Å and $c = 3.188$Å respectively. From Table 1, it can be seen that both $a$ and $c$ increase with annealing temperature increasing. It is reported that when the annealing temperature is close to 400 °C, there appear rapid decreases in density of vacant lattice sites, vacancy clusters, and local lattice disorders, and a rapid resumption of lattice parameters.[20] So it is reasonable for $\Delta a$ and $\Delta c$ to diminish with the annealing temperature increasing.

**Table 1.** The lattice constants of $Sn_{0.98}Ni_{0.02}O_2$ annealed at different temperatures.

| Annealing temperature /°C | $2\theta(110)$ | $2\theta(101)$ | $a$/Å | $\Delta a$/Å | $c$/Å | $\Delta a$/Å |
|---|---|---|---|---|---|---|
| 650 | 26.585 | 33.875 | 4.7379 | 0.0001 | 3.1863 | 0.0017 |
| 500 | 26.615 | 33.905 | 4.7326 | 0.0054 | 3.1840 | 0.0040 |
| 350 | 26.640 | 33.920 | 4.7287 | 0.0093 | 3.1833 | 0.0047 |

The morphologies of two typical samples annealed at 350 °C for 1 h are shown in Fig.3, in which (a) and (b) correspond to $x = 0.02$ and 0.05, respectively. As indicated in Fig.3, not only the grain size is reduced by nickel dopant, but also the grain shape is largely changed. Besides some spherical grains with a size of about 12 nm, sample with $x = 0.02$ is composed of some nano-rods with an average aspect ratio of about 10 and a length of about 100 nm. The nanorods were also observed in Co-doped $SnO_2$ powders.[15] However, the sample with $x = 0.05$ contains only spherical grains with a size of about 10 nm. The nano-particles are relatively well separated. As verified by XRD measurement, that the grain size can be reduced by nickel doping is also confirmed by TEM.

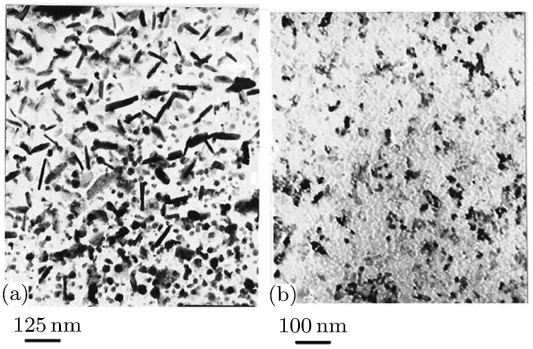



**Fig.3.** TEM images of $Sn_{1-x}Ni_xO_2$, with (a) $x = 0.02$ and (b) $x = 0.05$, respectively.

To determine the absorption band edge, we fit the absorption data to Eq.(2)[4]

$$(\alpha\hbar\omega)^2 \propto (\hbar\omega - E_g), \tag{2}$$

where $\hbar\omega$ is the photon energy, $\alpha$ is the absorption coefficient, and $E_g$ is the absorption band gap energy. $E_g$ is given by extrapolating the linear region to zero absorption. Figure 4 shows this fitting for the two typical samples annealed at 350 °C with $x = 0$ and $x = 0.05$, and the inset shows $E_g$ as a function of $x$.

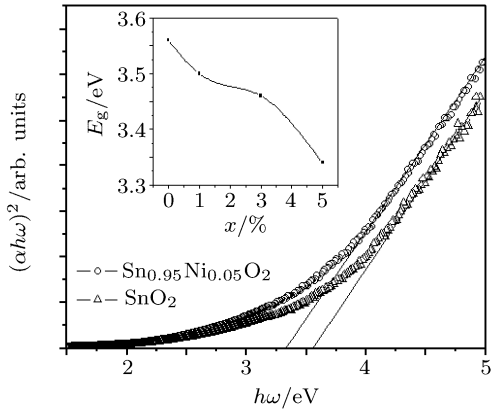



**Fig.4.** $(\alpha\hbar\omega)^2$ versus photo energy curve. The solid line is a linear fit to the experimental data. The inset shows the band gap energy as a function of nickel doping level $x$.

As determined in Fig.4, the band gap energies are 3.56 eV and 3.34 eV for samples with $x = 0$ and $x = 0.05$, respectively. Band gap energy shows a narrowing effect of nickel doping. The band gap narrowing with Fe-doping has also been observed,[21] however, there is no clear understanding of this phenomena. As the band gap energy increases with $x$ for $Zn_{1-x}Fe_xSe$ and $Zn_{1-x}Co_xSe$ but decreases with $x$ for $Zn_{1-x}Mn_xSe$,[16] the influence on band gap energy is different from that for various 3d transition metal dopants. In the case of $Sn_{1-x}Mn_xO_2$, the band gap increasing with $x$ for $x \leq 0.11$ is attributed to the hybridization between localized Mn d states located near the band gap and O p-like valence bands, and the decrease in the band-gap energy for higher $x$ is interpreted as originating from $SnO_2$–$MnO_2$ alloying effects (the band gap of MnO is about 2 eV).[22] The optical properties of such alloys have been studied by Barreau *et al.*[23] If A and B are semiconductors, the gap, when $x$A is present in $(1-x)$B, is given in the linear model often used, by

$$E = E_B - (E_B - E_A)x, \tag{3}$$

where $E_B$, $E_A$ and $E$ are the optical band gap values of B, A and the alloy $A_xB_{1-x}$, respectively. For our samples, since the band gap of NiO (3.54 eV)[24] is almost the same as that of pure $SnO_2$ (3.56 eV), the alloying effect due to NiO is so small that it can

be neglected. On the other hand, as confirmed by XRD measurements, the presence of nickel dopant inhibits crystallization, so there should be more amorphous $SnO_{2-x}$ phases in nickel doped $SnO_2$ than in pure $SnO_2$. As the band gap energy of amorphous $SnO_{2-x}$ phase is about 2.3 eV,[25] the alloying effect due to amorphous $SnO_{2-x}$ should be responsible for the band gap narrowing effect. To explore the amorphous $SnO_{2-x}$ effect on band gap energy, the band gap energy of $Sn_{0.95}Ni_{0.05}O_2$ as a function of annealing temperature is illustrated in Fig.5.

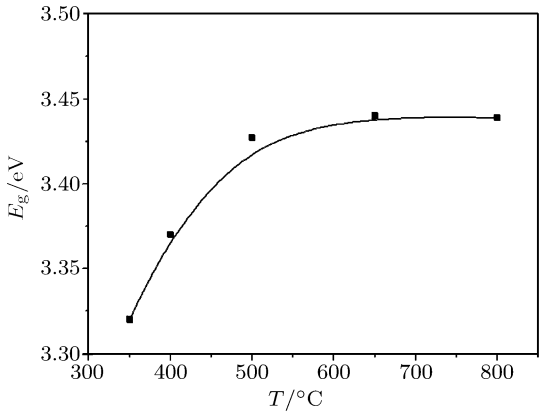



**Fig.5.** The band gap energy of $Sn_{0.95}Ni_{0.05}O_2$ as a function of annealing temperature.

With the annealing temperature increasing from 350 °C to 800 °C, the band gap broadens rapidly, and then increases slowly, and finally reaches a saturation value of 3.44 eV, a possible interpretation of which is that, with annealing temperature increasing, the quantity of amorphous $SnO_{2-x}$ decreases and finally vanishes, so that the band gap becomes larger and finally stabilized. Since the saturation value of band gap of 3.44 eV is still smaller than that of pure $SnO_2$ (3.56 eV), there should exist other factors contributing to the band gap narrowing effect. Kim *et al*[16] presented a sp-d hybridization model to interpret the band gap narrowing effect of $Zn_{1-x}Mn_xSe$. We think that the band gap energy modified in our samples should be partly related to this model, however, much work is still required to clarify the mechanism of the influence of 3d transition metal dopants on the band gap energy of $SnO_2$.

The PL spectrum can be used to conveniently investigate the structure and defect or impurity levels.[7] Figure 6 shows the room temperature PL spectra for pure $SnO_2$ and $Sn_{0.95}Ni_{0.05}O_2$ annealed at 350 °C for 1 h.

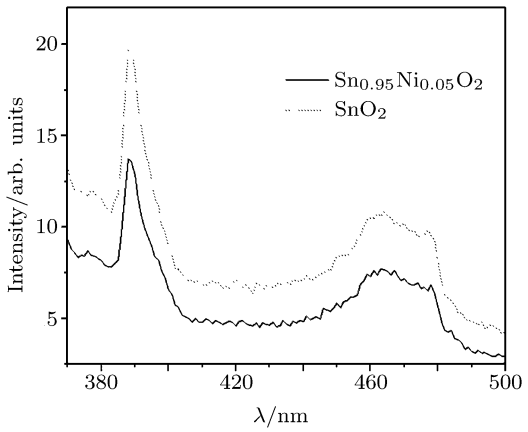



**Fig.6.** Room temperature PL spectrum of two typical samples with $x = 0$ and $x = 0.05$.

The PL spectra of both samples each show a strong UV emission peak at 389 nm (3.188 eV) and a broad blue emission near 470 nm (2.638 eV). Since the emissions are both lower than the band gaps of pure $SnO_2$ ($E_g$ = 3.56 eV) and $Sn_{0.95}Ni_{0.05}O_2$ ($E_g$ = 3.34 eV), the emissions cannot be assigned to the direct recombination of a conduction electron in the Sn 4p band and a hole in the O 2p valence band. This is similar to that illustrated by Gu *et al.*[5] The UV emission is reported in Refs.[3,6,7,26,27]. Kim *et al*[6] reported a weak peak at 3.13 eV, emitted from undoped $SnO_2$ at low temperatures and room temperature, and they thought that the origin of the peak was related to defects, or nanocrystalline grains, or defect levels associated with oxygen vacancies or tin interstitials resulting from the nanosize of the $SnO_2$ film. Thereafter, Jin *et al*[7] concluded that the PL peak at 3.1 eV was related to the structural defects and the peak at 2.4 eV was due to oxygen vacancies. Furthermore, Wang *et al*[3] reported that the oxygen vacancies did not play an important role in the origin of the UV emission at 3.16 eV of Sb doped $SnO_2$. As considered in our samples, the polycrystalline nano-$SnO_2$ grain assemblage has a large number of defects: vacancies of oxygen, vacancy clusters, and local lattice disorders at the interface and interior surface. It is difficult to identify the origins of UV and blue emission. It can be seen from Fig.6 that nickel doping does not change the peak positions, which is in good agreement with the result reported in Mn doped ZnO experiment.[28] The ratio of UV to blue emission, rather than the absolute PL intensity, is used for comparison since it is not possible to ensure that the same number of samples can be probed. The ratio of UV to blue emission decreases from 3.807 to 3.604 with $x$ increasing from 0 to 0.05. The annealing temperature does not change the PL

peak positions, but the ratio of UV to blue emission decreases with the annealing temperature increasing as shown in Fig.7. These PL phenomena are still not clearly understood now.

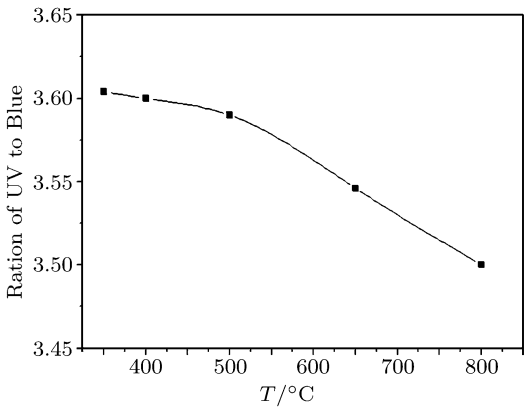



**Fig.7.** The ratio of UV to blue emission as a function of annealing temperature.

# 4. Conclusions

As a conclusion, $SnO_2$ nano-powder samples doped with nickel are successfully prepared. XRD measurements indicate that the grain size becomes larger and the structure of lattice grows better with nickel content decreasing. The obtained samples are polycrystalline with rutile structure of pure $SnO_2$ and no impurity phases existing. The band gap diminishes with the increasing of nickel content. The PL spectrum consists of a strong UV peak at 389 nm (about 3.188 eV) and a broad blue peak near 470 nm (about 2.638 eV). Nickel doping does not change the PL peak positions while the intensity ratio of UV/blue decreases. With the sintering temperature increasing, the ratio of UV/blue decreases, and the band gap increases and finally is saturated.

# References


[1] Nayral C, Viala E, Colliere V, Fau P, Senocq F, Maisonnat A and Chaudret B 2000 *Appl. Surf. Sci.* **164** 219

[2] Wang C, Appleby A J and Little F E 2002 *Solid State Ionics* **147** 13

[3] Wang Y H, Ma J, Ji F, Yu X H and Ma H L 2005 *J. Luminescence* **114** 71

[4] Yu B L, Zhu C S and Gan F X 1997 *Opt. Mater.* **7** 15

[5] Gu F, Wang S F, Song C F, Lu M K, Qi Y X, Zhou G J, Xu D and Yuan D R 2003 *Chem. Phys. Lett.* **372** 451

[6] Kim T W, Lee D U and Yoon Y S 2000 *J. Appl. Phys.* **88** 3759

[7] Jin J, Seong P C, Cha I C, Dong C S and Jin S P 2003 *Solid State Commun.* **127** 595

[8] Ji Z G, He Z J and Song Y L 2004 *Acta Phys. Sin.* **53** 4330 (in Chinese)

[9] Tesfamichael T, Will G, Colella M and Bell J 2003 *Nucl. Instr. Meth. Phys. Res.* B **201** 581

[10] Chopra K L, Major S and Pandya D K 1983 *Thin Solid Films* **102** 1

[11] Qu Y, Zhang X, Chen H, Gao J Y and Zhou D F 2005 *Chin. Phys.* **14** 1428

[12] Ogale S B, Choudhary R J, Buban J P, Lofland S E, Shinde S R, Kale S N, Kulkarni V N, Higgins J, Lanci C, Simpson J R, Browning N D, Sarma D S, Drew H D, Greene R L and Venkatesan T 2003 *Phys. Rev. Lett.* **91** 077205

[13] Fitzgerald C B, Venkatesan M, Douvalis A P, Huber S and Coey J M D 2004 *J. Appl. Phys.* **95** 7390

[14] Kuang A L, Liu X C, Lu Z L, Ren S K, Liu C Y, Zhang F M and Du Y W 2005 *Acta Phys. Sin.* **54** 2934 (in Chinese)

[15] Punnoose A and Hays J 2004 *Appl. Phys. Lett.* **85** 1559

[16] Kim Y D, Cooper S L, Klein M V and Jonker B T 1994 *Phys. Rev.* B **49** 1732

[17] Dinia A, Schmerber G, Pierron-Bohnes V, Mény C, Panissod P and Beaurepaire E 2005 *J. Magn. Magn. Mater.* **286** 37

[18] Safonova O V, Rumyantseva M N, Kozlov R I, Labeau M, Delabouglise G, Ryabova L I and Gaskov A M 2000 *Mater. Sci. Eng.* B **77** 159

[19] Rumyantseva M N, Gaskov A M, Ryabova L I, Senateur J P and Chenevier B 1996 *Mater. Sci. Eng.* B **41** 333

[20] Yu K N, Xiong Y, Liu Y and Xiong C 1997 *Phys. Rev.* B **55** 2666

[21] Coey J M D, Douvalis A P, Fitzgerald C B and Venkatesan M 2004 *Appl. Phys. Lett.* **84** 1332

[22] Park Y R and Kim K J 2003 *J. Appl. Phys.* **94** 6401

[23] Barreau N, Bernede J C, Marsillac S and Mokrani A 2002 *J. Cryst. Growth* **235** 439

[24] Sasi B, Gopchandran K G, Manoj P K, Koshy P and Rao P P 2003 *Vacuum* **68** 149

[25] Watanabe Y, Endo H, Semba H and Takata M 1994 *J. Non-Cryst. Solids* **178** 84

[26] Wang Y H, Ma J, Ji F, Yu X H, Zhang X J and Ma H L 2005 *Acta Phys. Sin.* **54** 1731 (in Chinese)

[27] Yu B L, Wu X C, Chen W J, Zou B S, Zhang G L and Tang G Q 1995 *Acta Phys. Sin.* **44** 660 (in Chinese)

[28] Roy V A L, Djurisic A B, Liu H, Zhang X X, Leung Y H, Xie M H and Gao J 2004 *Appl. Phys. Lett.* **84** 756